Materials Science-Poland
http://www.materialsscience.pwr.wroc.pl/
DOI: 10.2478/msp-2019-0044

Effect of the electrodeposition potential on the magnetic properties of FeCoNi lms

SETIA BUDI[1,] , SUKRO MUHAB[1], AGUNG PURWANTO[1], BUDHY KURNIAWAN[2], AZWAR MANAF[2,†]

[1]Department of Chemistry, Faculty of Mathematics and Sciences, Universitas Negeri Jakarta, Jl. Rawamangun Muka, Jakarta 13220, Indonesia

[2]

and potential are essential variables that should be adjusted to control kinetics of the deposition process. By altering the electrodeposition potential, microstructure and chemical composition of the transition metals alloys, such as CoNiCu [15] and CoNi [16], can be modified. This condition leads to significant changes in their magnetic properties [10, 16]. Since the magnetic properties of the FeCoNi also depend on its microstructure and composition, it is interesting to investigate the role of these electrodeposition variables on the electrodeposited FeCoNi films.

In our previous works [15, 16], the FeCoNi film was successfully electrodeposited on a flexible substrate of polyethylene terephthalate coated with indium tin oxide (ITO-PET). The using of a flexible substrate was motivated by the recent demand for flexible magnetic films due to the development of flexible electronic devices [17, 18]. Herein, we investigated the influence of electrodeposition potential on magnetic properties of the FeCoNi film electrodeposited on the ITO-PET substrate. The FeCoNi deposits obtained in this work demonstrated properties of typical soft magnetic alloys with low coercivity and high saturation which could be controlled through the applied electrodeposition potential. The relation between the applied potential, chemical composition and magnetic properties of the film was discussed.

2. Materials and method

The electrodeposition of FeCoNi was performed in sulfate electrolyte system, which was freshly prepared from analytical grade $FeSO_4\ 7H_2O$, $CoSO_4\ 7H_2O$, $NiSO_4\ 6H_2O$, H_3BO_3 precursors and the food grade $C_7H_4NNaO_3S\ 2H_2O$ chemical. The concentration of the electrolytes used in the electrodeposition process for the FeCoNi preparation is listed in Table 1. The electrodeposition was carried out under various electrodeposition potentials using EDAQ potentiostat of EA163 type in the potentiostatic mode. The substrate used in this work was polyethylene terephthalate coated with indium tin oxide (ITO-PET) with a sheet resistance of 20 Ω/sq supplied by Kintec. The coated ITO is amorphous phase composed of In_2O_3:SnO_2 at a ratio of 9:1 with a thickness of 180 nm. A platinum wire and Ag/AgCl acted as a counter and a reference electrode, respectively. The electrodeposition potential applied in the process was varied from −1.00 V to −2.00 V relative to Ag/AgCl electrode with the deposition time of 5 minutes. In this case, the electrodeposition processes were carried at potentials higher than the standard reduction potential of Fe^{2+} (−0.44 V), Co^{2+} (−0.28 V), and Ni^{2+} (−0.25 V) due to the co-deposition overpotential of the metal ions [19, 20].

Table 1. Concentration of the solution used as metal sources in the electrodeposition process.

Chemicals	Molarities [mol/L]
$FeSO_4\ 7H_2O$	0.010
$CoSO_4\ 7H_2O$	0.020
$NiSO_4\ 6H_2O$	0.170
H_3BO_3	0.400
$C_7H_4NNaO_3S\ 2H_2O$	0.008

The mean crystallite size of FeCoNi films was evaluated by Panalytical EMPYREAN X-ray diffractometer (XRD) employing CuK_α radiation (λ = 1.541874 Å). The obtained XRD patterns were compared to the standard pattern of FeCoNi alloy from Crystallography Open Database (COD) number 96-900-00900 [21]. The mean crystallite size of the FeCoNi films was then determined by Rietveld refinement method using HighScore Plus software. The mass content of Fe, Co and Ni in the deposits was quantitatively determined using a Shimadzu AA7000 atomic absorption spectrometer (AAS). Magnetic properties were measured for 4 mm × 4 mm FeCoNi films using LakeSore 7404 vibrating sample magnetometer (VSM) equipped with a magnetic field (H) up to 900 kA/m.

3. Results and discussion

X-ray diffraction patterns of the FeCoNi alloy films deposited at various negative potentials are compared in Fig. 1. Obviously, all patterns show a diffraction peak at a diffraction angle 2θ of 44.17° related to (1 1 1) plane

of FeCoNi. The sample prepared at a low pote tial (1.00 V vs. Ag/AgCl) shows additional peaks corresponding to the diffraction peaks of ITO an PET substrates [22]. Since all of the FeCoNi lm were electrodeposited in the same deposition tin the pattern was then attributed to very thin depo due to the low deposition rate of Fe, Co and Ni 1.00 V vs. Ag/AgCl and hence, it allowed the X-ray to reach the substrate. Nevertheless, these a tional peaks vanished in the lms obtained at mo negative values of the electrodeposition potent (1.10 V to 2.00 V vs. Ag/AgCl). It is also noted that another diffraction peak appears at a other diffraction angle 51.57 which corresponds to the (2 0 0) plane of FeCoNi [21]. This peak was observed in all samples prepared through electrodeposition at potential ranging from 1.50 V to 2.00 V vs. Ag/AgCl. All diffraction patterns shown in Fig. 1 have been matched with the results on the phase structure evaluation of mechanically alloyed FeCoNi reported by Pikula [3]. The formation of FCC solid solution of FeCoNi alloy in the lm samples obtained in the current work was then con rmed. Additionally, the patterns shown in Fig. 1 are characterized by broadened peaks re ecting the existence of ultra ne crystallites in the lms. The mean crystallite size was found in a small range between 11 nm and 15 nm. Hence, there is no substantial in uence of electrodeposition potential on the mean crystallite size of the FeCoNi lms. However, when the mean crystallite size of FeCoNi lms is compared with that obtained by mechanical alloying technique [3], it is realized that the mean crystallite size of the current alloy lms is much ner than that of mechanically alloyed FeCoNi.

The atomic fraction (at.%) of Fe, Co and Ni contained in the FeCoNi alloy lms deposited at different electrodeposition potentials is plotted in Fig. 2a. The plot indicates that the electrodeposition potentials applied during the lm deposition control the atomic fraction of Fe, Co and Ni atoms. The more negative potential is applied, the more abundant concentration of Ni is in the lm. In addition, it can be seen that Fe and Co concentrations were found to decrease at more negative potentials. In this case, Fe content decreased from 22.68 at.% at a potential of 1.10 V vs. Ag/AgCl to 10.18 at.% at a potential of 2.00 V vs. Ag/AgCl. Similarly, the Co content decreased from 40.77 at.% to 20.70 at.%. Consequently, the alloy was enriched with Ni as the applied potential was getting more negative. Fig. 2b shows the plots of Ni/Fe and Ni/Co atomic ratios versus the applied potential. As the potential increases negatively from 1.00 V to 1.75 V vs. Ag/AgCl, the Ni/Fe and Ni/Co ratios increase almost linearly. Nevertheless, at a potential lower than 1.75 V vs. Ag/AgCl, no further increase is noticed. The difference between the ratio values of Ni/Fe and Ni/Co must be related to the standard potential of Ni^{2+}.

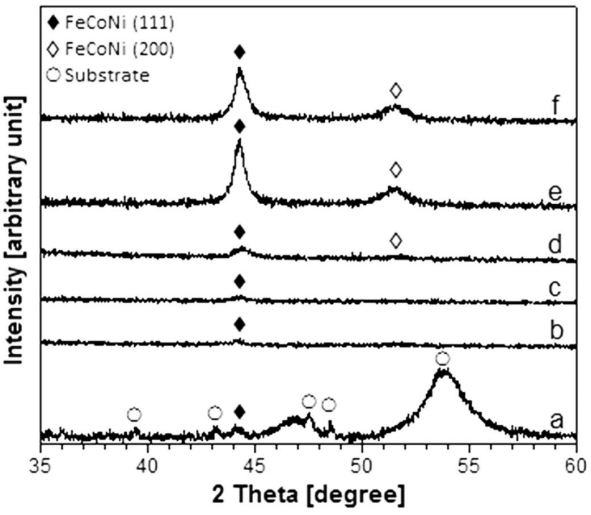

Fig. 1. X-ray diffraction patterns of the FeCoNi lms deposited at electrodeposition potentials of (a) 1.00 V, (b) 1.10 V, (c) 1.30 V, (d) 1.50 V, (e) 1.75 V and (f) 2.00 V vs. Ag/AgCl.

The relatively high content of Co and Fe in the lm obtained from electrolyte with high Ni^{2+} ions concentration, especially observed at 1.00 V vs. Ag/AgCl, indicates anomalous co-deposition in the electrodeposition process. Anomalous co-deposition is a phenomenon showing a high deposition preference of less noble metal, namely Fe and Co, compared to more noble metal Ni. However, at more negative potential (1.10 V vs. Ag/AgCl) the Ni content was found to increase gradually when the electrodeposition potential shifted to more negative ones. It can

be assumed that the anomalous co-deposition cha acteristics decreased at more negative potentia This results could be attributed to the high over potential of Ni [19, 23] which leads to rising the deposition rate of Ni at more negative potential. I was also found that the change of Co content at di ferent electrodeposition potentials is similar to tha of Fe (Fig. 2a). In fact, the standard reduction po tential of Co is closer to that of Ni rather than Fe This case can be related to the composition rati value (CRV) of Co that exhibits similar behavior to that of Fe [24].

It was recorded in our previous report that al though the standard reduction potential of Ni^{2+} is lower than that of both Fe^{2+} and Co^{2+}, the Ni^{+2} ion possesses the highest overpotential among the investigated metal ions [14]. The high overpoten tial of Ni^{+2} has led to a higher deposition rate of Ni at a high electrodeposition potential difference compared with those of Fe and Co. Consequentl the atomic fraction of Ni in the lm is much higher than that of Fe and Co. In Fig. 2b, the atomic ratio between Co and Fe was also plotted. There is a most no change in the atomic ratio between Co ar Fe atoms with the applied potential in the range o 1.1 V to 2.00 V vs. Ag/AgCl. However, at a potential of 1.00 V vs. Ag/AgCl, the atomic fractions of the three components are mostly equal to each other with the composition ratio about 1:1:1.

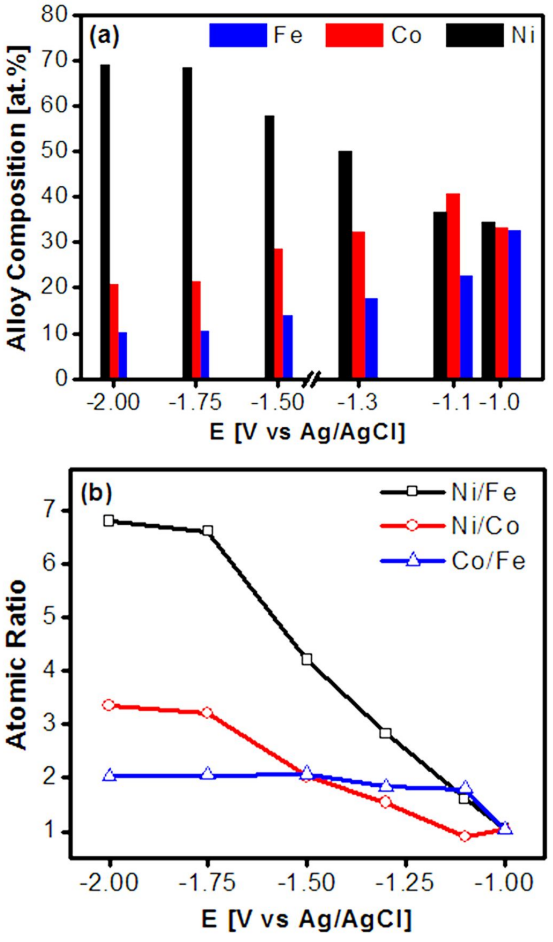

Fig. 2. Atomic composition of Ni, Co and Fe (a) and atomic ratio Ni/Fe, Ni/Co, Co/Fe values (b) in FeCoNi lms prepared at different electrodeposition potentials.

Fig. 3a compares the hysteresis loops of the FeCoNi lms prepared at potentials of 1.00 V, 1.30 V and 1.75 V. Evaluation of magnetic properties of FeCoNi alloy lms was carried out in two different directions. The two directions were marked as IP (in-plane) and OP (out-plane) which refer to parallel and perpendicular to the direction of the applied magnetic eld, respectively. Hysteresis loops shown in Fig. 3a are typical of that of soft magnetic lms. The saturation magnetization state is achieved mostly at a relatively small external magnetic eld. This result is con rmed by FeCoNi lms prepared at the electrodeposition potentials of 1.00 V, 1.30 V and 1.75 V vs. Ag/AgCl. For the latter, a slightly higher magnetic eld was required to achieve the saturation state due to the anisotropy characteristic of that sample. Although the sample shows anisotropy characteristics, the saturation magnetization value of each sample is the same for both directions (IP and OP). Generally, the magnetic anisotropy of the sample can be associated with the crystalline anisotropy and shape anisotropy. The crystalline anisotropy in the sample would take effect when crystallites of magnetic phase are oriented to a preferred direction. For this case, it still cannot be confirmed if the preferred orientation of the crystallites can induce the magnetic anisotropy of the FeCoNi lms deposited at different co-deposition potentials. However, since the length L to thickness T ratio of the lm (L:T) is in the range of 16000 to 30000, then the magnetic anisotropy observed by the sample prepared at an electrodeposition

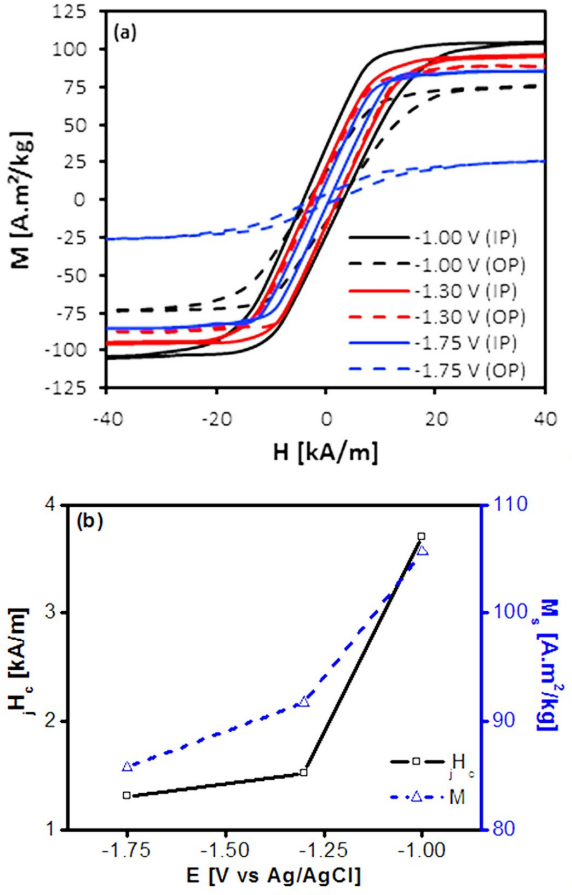

Fig. 3. Hysteresis loops of FeCoNi lms (a) prepared at various electrodeposition potentials and (b) the corresponding intrinsic coercivity ($_jH_c$) and saturation magnetization (M_s) values obtained from IP loops.

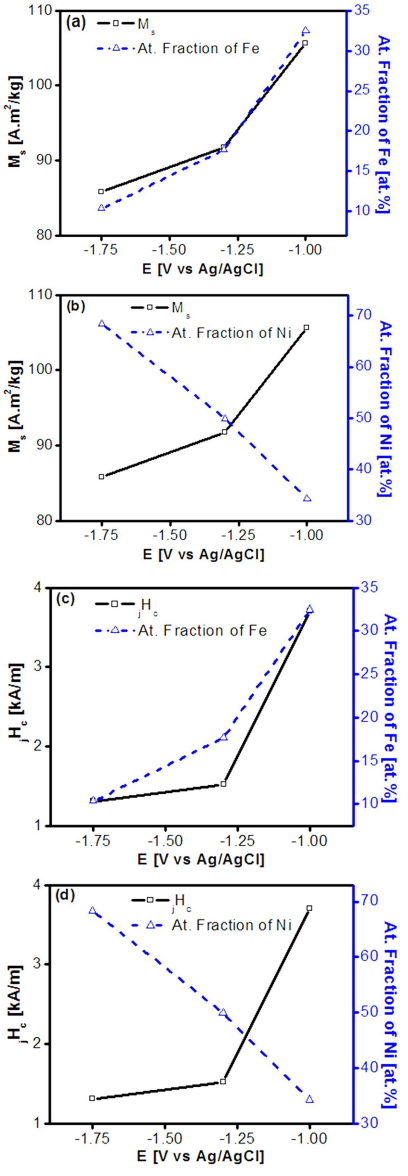

Fig. 4. Composition dependent intrinsic coercivity ($_jH_c$) and saturation magnetization (M_s) values of FeCoNi lms measured in IP directions

potential of 1.75 V vs. Ag/AgCl is more likely due to a shape anisotropy of the sample.

Both saturation magnetization and coercivity values of the samples increased as the electrodeposition potential became less negative. The increase in saturation magnetization value is due to the higher content of Fe and Co atoms, and lower content of Ni in the FeCoNi alloy. This condition was followed by an increase in the corresponding coercivity.

In the previous discussion, we have shown that the applied potential during electrodeposition of FeCoNi lms caused a change in the composition. The variation in the composition of the alloy lm resulted in a modi cation in the magnetic properties of FeCoNi lms. The plots of M_s and $_jH_c$ values of FeCoNi lms of various compositions are shown in Fig. 4. It shows an increase in both M_s and $_jH_c$ values with an increase in Fe content in the FeCoNi lm (Fig. 4a and 4c). The M_s and $_jH_c$ values get increased with a decrease in Ni content (Fig. 4b and 4d). The reason for these results is that the net magnetic moment of Fe atom (2.22 μ_B) [25]

is the highest among the three transition metals followed by Co (1.72 μ_B) and Ni (0.60 μ_B) [25]. It is known that magnetization and coercivity are properties which depend on microstructure and chemical composition of materials [5, 10, 26]. However, since there is no meaningful change in the crystallite size of the electrodeposited FeCoNi alloys, the changes in their magnetic characteristics could be solely attributed to the chemical composition of the alloy. In this case, once again the increase in Fe and Co content resulted in the increasing saturation magnetization. However, the change in coercivity is more likely due to the change in the magnetocrystalline constant of the FeCoNi.

4. Conclusion

This study demonstrates the in uence of the applied potential on magnetic properties of electrodeposited FeCoNi lms. The magnetic properties were found to be solely dependent on the atomic fraction of Fe, Co and Ni atoms, which was successfully controlled through the adjustment of the electrodeposition potential because there was no signi cant change found in the crystallite size. The FeCoNi lms possess excellent soft magnetic properties with the highest $_sM$ value of 105 Am^2/kg and $_jH_c$ value of 3.7 kA/m obtained at the electrodeposition potential of 1.00 V vs. Ag/AgCl with the Fe, Co and Ni composition close to 1:1:1.

Acknowledgements

This work was supported by the Universitas Negeri Jakarta and the Directorate General of the Higher Education (RISTEKDIKTI) Republic of Indonesia through the Research Grant of Penelitian Terapan with the Contracts No. 60/SP2H/DRPM/LPPM-UNJ/II/2018 and No. 27/SP2H/DRPM/LPPM-UNJ/III/2019.

References

[1] OSAKA T., TAKAI M., HAYASHI K., OHASHI K., Nature, 392 (1998), 796.
[2] LUCIU I., DUDAY D., CHOQUET P., PERIGO E.A., MICHELS A., WIRTZ T., Appl. Surf. Sci. 389 (2016), 578.
[3] PIKULA T., OLESZAK D., MAREK P., J. Magn. Magn. Mater., 320 (2008), 413.
[4] FU P., CHEN G., XU Y., CAI P., WANG X.H., Mater. Sci.-Poland, 30 (2012), 259.
[5] RAANAEI H., ESKANDARI H., MOHAMMAD-HOSSEINI V., J. Magn. Magn. Mater. 398 (2016), 190.
[6] BAGHBADERANI H.A., SHARA S., CHERMAHINI M.D., Powder Technol. 230 (2012), 241.
[7] SHAKYA P., COX B., DAVIS D., J. Magn. Magn. Mater. 324 (2012), 453.
[8] DUAN Y., ZHANG Y., WANG T., GU S., XIN L., XINGZUN L.V., Mater. Sci. Eng. B-Adv. 185 (2014), 86.
[9] ALI G.A.M., YUSOFF M.M., NG Y.H., LIM H.N., CHONG K.F., Curr. Appl. Phys. 15 (2015), 1143.
[10] DAUD A.R., BUDI S., RADIMAN S., Sains Malaysiana, 40 (2011), 1019.
[11] HANAFI I., DAUD A.R., RADIMAN S., GANI M.H.A., BUDI S., J. Phys. Conf. Ser. 431 (2013), 1.
[12] HANAFI I., DAUD A.R., RADIMAN S., Port. Electrochim. Acta, 35 (2017), 1.
[13] TALIK E., GUZIK A., ZAJDEL P., LIPIŃSKA L., BARAN M., SZUBKA M., Mater. Res. Bull. 83 (2016), 56.
[14] AKBULUT S., AKBULUT A., ÖZDEMIR M., YILDIZ F., J. Magn. Magn. Mater. 390 (2015), 137.
[15] BUDI S., HAFIZAH M.E., MANAF A., AIP, 1746 (2016), 020012-1.
[16] BUDI S., KURNIAWAN B., MOTT D.M., MAENOSONO S., UMAR A.A., MANAF A., Thin Solid Films, 642 (2017), 51.
[17] XIAO L., CHEN Z., FENG C., LIU L., BAI Z.-Q., WANG Y., QIAN L., ZHANG Y., LI Q., JIANG K., FAN S., Nano Lett., 8 (2008), 4539.
[18] LEE H., WANG L., BAIN J.A., LAUGHLIN D.E., IEEE T. Magn, 41 (2005), 654.
[19] BUDI S., DAUD A.R., RADIMAN S., UMAR A.A., Appl. Surf. Sci. 257 (2010), 1027.
[20] MATLOSZ M., J. Electrochem. Soc. 140 (1993), 2272.
[21] GRAZULIS S., CHATEIGNER D., DOWNS R.T., YOKOCHI A.F.T., QUIRÓS M., LUTTEROTTI L., MANAKOVA E., BUTKUS J., MOECK P., LE BAIL A., J. Appl. Crystallogr. 42 (2009), 726.
[22] VEITH M., BUBEL C., ZIMMER M., Dalt. Trans, 40 (2011), 6028.
[23] DOLATI A., SABABI M., NOURI E., GHORBANI M., Mater. Chem. Phys. 102 (2007), 118.
[24] YANG Y., Int. J. Electrochem. Sci. 10 (2015), 5164.
[25] CULLITY B.D., GRAHAM C.D., Introduction to Magnetic Materials, John Wiley & Sons, New Jersey, 2008.
[26] VELIGATLA M., KATAKAM S., DAS S., DAHOTRE N., GOPALAN R., PRABHU D., BABU D.A., CHOI-YIM H., MUKHERJEE S., Metall. Mater. Trans. A 46 (2015), 1019.

Received 2018-04-07
Accepted 2018-11-12